Organic Geochemistry 79 (2015) 65–73

Contents lists available at ScienceDirect

Organic Geochemistry

journal homepage: www.elsevier.com/locate/orggeochem

Influence of temperature and C_4 abundance on *n*-alkane chain length distributions across the central USA

Rosemary T. Bush [a,*], Francesca A. McInerney [a,b]

[a] Dept. of Earth and Planetary Sciences, Northwestern University, 2145 Sheridan Road, Evanston, IL 60208, USA
[b] Sprigg Geobiology Centre, Environment Institute and the School of Earth and Environmental Sciences, University of Adelaide, Adelaide, South Australia 5005, Australia

ARTICLE INFO

Article history:
Received 10 July 2014
Received in revised form 24 November 2014
Accepted 5 December 2014
Available online 16 December 2014

Keywords:
Leaf wax *n*-alkanes
Temperature
Paleoclimate
Paleoenvironment

ABSTRACT

The distributions of long chain *n*-alkanes are often utilized as plant-derived paleoenvironmental proxies. However, there is debate regarding the degree to which photosynthetic pathway, temperature and/or hydrology drive the variation in chain length distribution observed among different environments. In order to assess the influence of temperature and photosynthetic pathway on plant *n*-alkanes, this study examined *n*-alkane chain length distributions in plants and soils along a transect across mid-continental USA spanning > 20 °C mean annual temperature with a limited range of mean annual precipitation. We found that (i) longer chain length in plants and soils correlated with higher growing season temperature, with relative humidity also a possible driver, (ii) soils exhibited a stronger correlation with temperature than did individual plants, which may reflect the averaging of plant input to soils and (iii) average chain length values in soils did not correlate with the predominance of C_4 plants. The data suggest that the spatial and temporal variation in chain length distributions observed in studies of sediment archives may be driven in large part by growing season temperature and/or aridity rather than photosynthetic pathway (C_3 or C_4). The findings call for further research into the mechanisms and effects of leaf wax composition on water permeability under different environmental conditions, the relationship between leaf wax *n*-alkanes and relative humidity, and the incorporation of *n*-alkanes into soils and sediments.

1. Introduction

Long chain *n*-alkanes (C_{21}–C_{39}) are synthesized as part of the epicuticular leaf wax and are typically long-lived in the sedimentary record (Eglinton and Hamilton, 1967). As a result, they serve as plant biomarkers and valuable paleoclimate and paleoenvironment proxies. Most paleoenvironmental applications use the stable isotope ratios of *n*-alkanes (Castañeda and Schouten, 2011; Sachse et al., 2012), but chain length distributions have been hypothesized to reflect source plant groups or climate drivers such as temperature and aridity (Bush and McInerney, 2013 and references therein). Drivers of chain length also form an important part of consideration of the stable isotope values from sediment archives, for example when considering different chain lengths contributed by C_3 and C_4 vegetation (Wang et al., 2013). Data from a broad survey of modern plants do not support a direct link between chain length and most major terrestrial plant types, with the notable exceptions of aquatic plants and *Sphagnum* moss (Bush and McInerney, 2013). Temperature and aridity have been posited, but much of the evidence relating *n*-alkane chain length to climate variables has been relatively indirect, coming from studies of *n*-alkanes in atmospheric dust, marine surface sediments, or stratigraphic sections (e.g. Kawamura et al., 2003; Rommerskirchen et al., 2003; Castañeda et al., 2009), with only a few recent studies demonstrating correlations between chain length and temperature or aridity in living plants (Hoffmann et al., 2013; Tipple and Pagani, 2013). In studies of sediment archives, shifts in chain length are often concurrent with large shifts in climate and the local plant community (e.g. Brincat et al., 2000; Schwark et al., 2002), leading to potential conflation of climate and plant type as the direct driver. Furthermore, although studies have shown that C_4 grasses generally produce longer chain lengths than C_3 grasses (Rommerskirchen et al., 2006b), C_4 plants thrive in hot, dry conditions while C_3 plants are favored by cooler, wetter conditions. Thus, comparison of *n*-alkanes from C_3 and C_4 plants can conflate environment and photosynthetic pathway. In fact, C_3 plants from dry savanna environments, where C_4 grasses are predominantly found, produce long chain length distributions more similar to those of C_4 grasses than C_3 plants in wet rainforests (Vogts et al., 2009). The

* Corresponding author at: Dept. of Civil & Environmental Engineering & Earth Sciences, University of Notre Dame, 156 Fitzpatrick Hall, Notre Dame, IN 46556, USA. Tel.: +1 (832) 588 7290.
E-mail address: rbush@nd.edu (R.T. Bush).

http://dx.doi.org/10.1016/j.orggeochem.2014.12.003
0146-6380/

correlations between *n*-alkane chain length from sediment archives and shifts in environmental variables are promising, but the meaning of the shifts is unclear and can only be elucidated via tests using modern plants and soils.

The goal of this study was to assess the degree to which temperature, relative humidity and C_4 abundance correlated with *n*-alkane chain length concentration and distribution in plants and soils across a large spatial scale. We sampled 70 sites across a ca. 2700 km transect through the central USA, from the Minnesota–Canada border in the north to the Texas–Mexico border in the south. In the central US, temperature generally varies along a latitudinal gradient, while precipitation changes with longitude, which allows sampling a large natural temperature gradient while largely controlling annual precipitation (Fig. 1). There is also a strong gradient in the proportion of C_4 plants through the area, as the proportion of C_4 plants increases with decreasing latitude (Teeri and Stowe, 1976; Still et al., 2003). We utilized climate data from the PRISM Climate Group (Section 2.4) for temperature and precipitation measurements and measured carbon isotope values of soil organic matter (OM) as a proxy for the proportion of C_4 plants (Tieszen et al., 1997). Within this framework, we could examine the influence of climate on the concentration and distribution of plant-derived *n*-alkanes, which is crucial for applying them as a paleoclimate proxy.

2. Methods

2.1. Samples and locations

Leaf and soil samples were collected in September 2012 from 70 locations along a transect from International Falls, Minnesota to Brownsville, Texas (Fig. 1). To minimize soil disturbance and the effect of human activity, sites were selected in state parks and wildlife management areas. Due to the paucity of protected natural areas through the central Great Plains, these sites were supplemented by sampling from small rural cemeteries, which can provide minimally disturbed areas for native plant species to grow in regions otherwise dominated almost exclusively by cultivated land (Sorensen and Holden, 1974; Gustafson et al., 2005). Natural area sites were selected, where possible, to balance accessibility with minimizing anthropogenic effects and were typically away from roads and adjacent (5–20 m) to hiking or access trails. Cemetery site selection was more limited, but effort was made to locate least disturbed areas, e.g. oldest, non-mowed and/or perimeter sections and beside (rather than before or behind) visible grave markers. Site information is reported in the Supplementary material (Appendix A). The transect covers a range of 20.2 °C in mean annual temperature and was devised to restrict the variation in annual precipitation as much as possible. The latter ranges from 559 to 736 mm, with a mean of 667 mm, but it should be noted that the seasonality changes from summer-wet at the north end to proportionally more autumn and winter precipitation in the south. Sampling sites span from mixed temperate forest in northern Minnesota, tall grass and mixed grass prairies through the central states, to savanna and sub-tropical forest in southernmost Texas.

For soil samples, surface duff (if present) was removed and 60 ml soil collected with a hand trowel from 2 to 8 cm depth. They were stored in glass jars with a liner of Al foil under the lid and oven dried at 50 °C. Glass jars and foil liners were ashed at 420 °C prior to sample collection. Plant samples were collected and stored in stapled brown paper bags or in a plant press and were allowed to air dry for several days. Soil samples were sieved through 2 mm mesh, and root and stem pieces were removed.

2.2. Lipid extraction and quantification

Lipids were extracted from ca. 5 g soil or 0.1–0.4 g dry leaf sample in 30 ml dichloromethane (DCM):MeOH (9:1 v/v) using microwave extraction (MARS-X) with a ramp to 100 °C (held 15 min) and minimum cooling time 30 min. Each total lipid extract was concentrated under a stream of dry N_2. Non-polar lipids, including

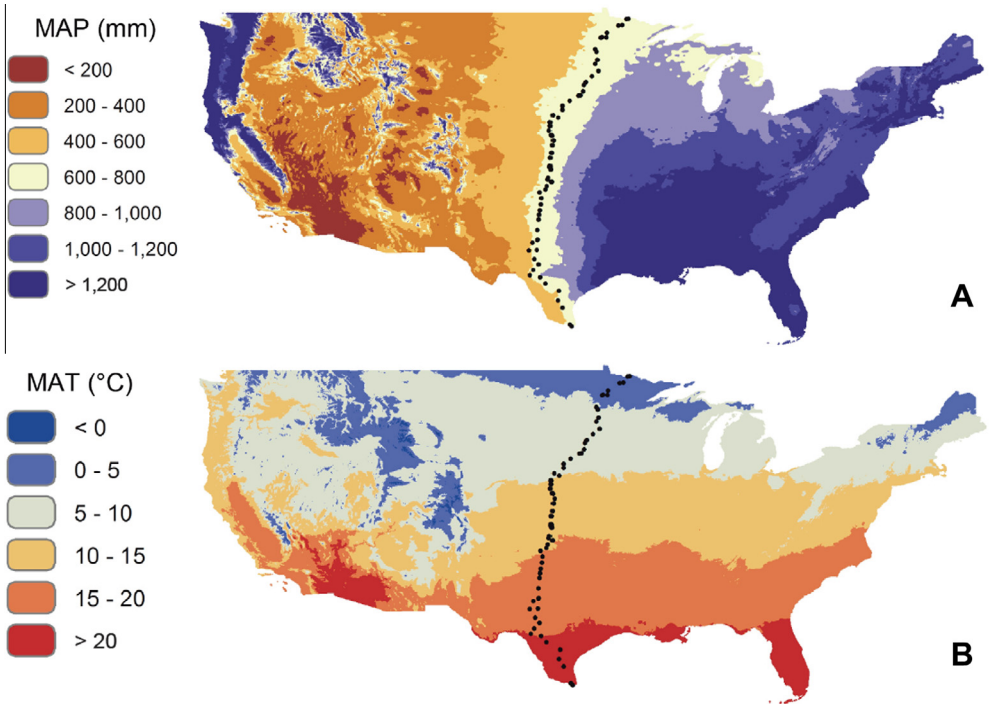

Fig. 1. Sample locations (black points) showing (A) mean annual precipitation (MAP) and (B) mean annual temperature (MAT), using data from PRISM climate normals, 1981–2010.

n-alkanes, were separated from the polar lipids via short column silica gel chromatography, using ca. 1 g activated silica gel in a Pasteur pipette plugged with glass wool and 4 ml hexane. Polar lipids were eluted in 4 ml 1:1 DCM:MeOH. Five plant samples required further separation of saturated from unsaturated non-polar lipids via elution through a short column of silica gel with 5% $AgNO_3$ (ca. 1 g), eluting saturated lipids with 4 ml hexane and unsaturated lipids with 4 ml EtOAc. Saturated lipids were again concentrated via evaporation with dry N_2. Each sample was dissolved in hexane and an internal standard added (1–1′ binaphthyl, 10 ng/ml in hexane; Sigma–Aldrich) prior to analysis using gas chromatography–mass spectrometery (GC–MS; Medeiros and Simoneit, 2007). The GC instrument (Thermo Scientific Trace GC Ultra) was equipped with a 15 m × 0.25 mm i.d. column (Thermo TR-5 ms SQC) and interfaced with a quadrupole mass spectrometer for identification (Thermo Scientific DSQII). The samples were simultaneously injected onto a separate column (with the same specifications) via a second inlet in the same GC instrument and analyzed via flame ionization detection (FID) for abundance. The GC oven temperature program was: 100 °C (held 2 min) to 320 °C (held 5 min) at 11 °C/min. Quantification used the internal standard, calibrated to a homologous series of *n*-alkanes from C_{21} to C_{40} (Fluka, Sigma–Aldrich). Sample chain length ranged from C_{16} to C_{39}. Average chain length (ACL) was limited to C_{21} to C_{39}, recognized as being predominantly from plants (Bush and McInerney, 2013). It was calculated as follows:

$$\mathrm{ACL} = \frac{(21C_{21} + 23C_{23} + \cdots + 39C_{39})}{(C_{21} + C_{23} + \cdots + C_{39})},$$

where C_x is the abundance of the chain length with *x* carbons. Carbon preference index (CPI) was calculated using the abundances of odd and even chain lengths from C_{21} to C_{39}, following Marzi et al. (1993):

$$\mathrm{CPI} = \frac{(C_{21} + C_{23} + \cdots + C_{37}) + (C_{23} + C_{25} + \cdots + C_{39})}{2 \times (C_{22} + C_{24} + \cdots + C_{38})}.$$

2.3. Soil organic carbon (OC) content and $\delta^{13}C$ measurements

Sub-samples of sieved soil were ground and treated to remove carbonate using 0.5 N HCl for 1 h, repeated until all carbonate had been removed (via one additional acid treatment after the last rinse that generated visible bubbles) and then rinsed with deionized water until neutral. Samples were then lyophilized and weighed into Sn boats for analysis of C content and $\delta^{13}C$ values using an elemental analysis (EA) instrument (Costech Analytical Technologies) coupled via a Conflo IV interface to an isotope ratio mass spectrometry (IRMS) instrument (Thermo Finnigan Delta V Plus) at Northwestern University. EA used an oxidation reactor with Cr_2O_3 and silvered Co_3O_4 at 1020 °C, a reduction reactor with reduced Cu wires at 650 °C and a 4 m chromatography column at 65 °C. Isotope values were calibrated using certified standards including Acetanilide #1 and Urea #2 (A. Schimmelmann, Indiana University), IAEA-600 Caffeine and IAEA-CH3 Cellulose. They are reported relative to Vienna Peedee Belemnite (VPDB). Each sample was run in duplicate at a minimum. Average precision for total OC (TOC) content was better than ± 0.24% (1 σ) of measured values and average precision for $\delta^{13}C$ values was ± 0.2‰ (1 σ).

2.4. Climate estimates

Temperature and precipitation estimates, including monthly and annual averages for precipitation and for mean, minimum and maximum temperature, for the contiguous USA come from the PRISM Climate Group climate normals dataset, 1981–2010 (available at http://www.prism.oregonstate.edu). The PRISM datasets are modeled from physiographic data and climate stations across the conterminous USA at a resolution of 4 km (Daly et al., 2008). Average relative humidity (RH) was calculated separately for the months of June, July and August as well as annual RH over the same 30 yr period using monthly dewpoint temperatures from PRISM:

$$\mathrm{RH}\ (\%) = 100 \times \frac{e^{\frac{17.269 \times T_d}{237.3 + T_d}}}{e^{\frac{17.269 \times T}{237.3 + T}}},$$

based on Teten's formula for vapor pressure, where T_d is the monthly dewpoint temperature and *T* the monthly mean air temperature. All data are also provided in the Supplementary material (Appendix A). All analyses were performed with STATA IC 11.1.

3. Results

3.1. Soil TOC and $\delta^{13}C$ values

TOC (wt%) and $\delta^{13}C$ values for soil samples (n = 70) are reported in the Supplementary material (Appendix A). Average TOC was 3.1%, ranging from 0.3% to 11.7%. There was no correlation between TOC and latitude; $\delta^{13}C$ values ranged from −29.1‰ to −14.3‰, with the most negative values confined to the northern latitudes, and mixed values at middle and southern latitudes that largely reflected the input of C_4 plants (predominantly grass) to soil OM (Fig. 2). Although fractionation during the decay of soil OM is known to increase its $\delta^{13}C$ value with depth (Melillo et al., 1989; Buchmann et al., 1997), leaf litter and soil OM $\delta^{13}C$ values are highly correlated (Balesdent et al., 1993). The shallow soil depth at which the samples in this study were collected also minimized this potential bias, especially in comparison with the large range of measured $\delta^{13}C$ values. For comparison, Tieszen et al. (1997) reported soil $\delta^{13}C$ values of ca. −14‰ at 100% C_4 cover and ca. −24‰ at 0% C_4 cover in a study of Great Plains grasslands.

3.2. n-Alkane concentration and CPI values

Soil *n*-alkane concentration ranged from 0.4 to 27.5 μg/g sediment ($\bar{x}$ = 3.6 μg/g); concentration was much higher in plant samples, ranging from 61.4 to 7115 μg *n*-alkane/g dry leaf ($\bar{x}$ = 507.2 μg/g). Soil *n*-alkane content correlated with TOC (log–log regression, R^2 0.37, $p < 0.001$), suggesting that local plant matter was a source for both *n*-alkanes and TOC. Although the correlation is significant, the low strength likely reflects the multiple

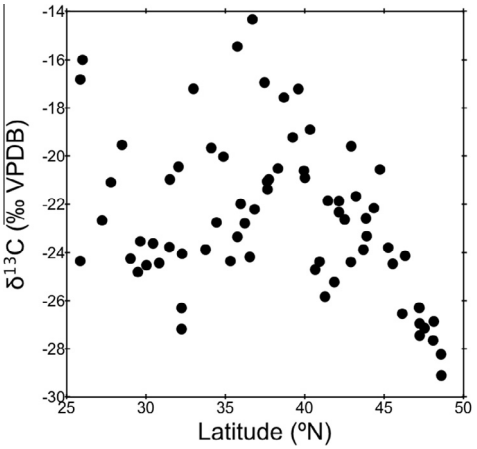

Fig. 2. Soil OC $\delta^{13}C$ values by latitude (n = 70).

inputs to soil OM, including microbial and fungal communities, while the long chain *n*-alkane source is likely almost entirely vascular plants. Soil *n*-alkane content did not significantly correlate with latitude, mean annual temperature, annual precipitation or soil $\delta^{13}C$ value. For soils, CPI values ranged between 2.4 and 10.0 ($\bar{x}$ = 5.7), well within the range of plant-derived CPI values (Bush and McInerney, 2013). Plant CPI values were between 2.1 and 16.7 ($\bar{x}$ = 6.3). Mean soil CPI was not significantly different from mean plant CPI in an unpaired Student's *t*-test (p 0.091). Soil CPI values did not correlate with soil TOC, latitude, mean annual temperature, annual precipitation or soil $\delta^{13}C$ values (for all regressions, $p > 0.01$ and $R^2 < 0.10$). Similarly, plant CPI values did not correlate with latitude, mean annual temperature, or mean annual precipitation ($p > 0.01$ and $R^2 < 0.10$).

3.3. n-Alkane ACL values and climate

Soil ACL values ranged between 27.6 and 32.8 ($\bar{x}$ = 30.3) and plant values between 26.4 and 31.7 ($\bar{x}$ = 29.4). Soil values correlated significantly with mean annual temperature (Fig. 3, black symbols; linear regression R^2 0.41, $p < 0.001$). They also correlated significantly with average seasonal temperature, with seasons calculated as an average of three months each: spring (March, April, May), summer (June, July, August), autumn (September, October, November) and winter (December, January, February). Table 1 shows the linear regression results for all soils for each season as well as mean annual temperature, with results separated by whether soils were collected from cemetery sites or sites in protected natural areas. Linear regression results for plant samples (n = 54) by temperature are also shown in Table 1. For soil samples, regression results were significant for all correlations and summer was the most strongly correlated of all four seasons (Fig. 3, gray symbols). Across all seasons, and for mean annual temperature, natural area soils correlated more strongly with temperature than cemetery samples. Fig. 4 presents ternary diagrams of soil *n*-alkane distributions using C_{27} and greater, with the sites color coded by mean annual temperature. Two attributes of the relationship between temperature and *n*-alkane chain length are apparent in Fig. 4. First, the increase in relative abundance with increasing temperature is greater for C_{33} and C_{35} than for C_{31}, likely because C_{31} is relatively abundant compared with the longer chain lengths. Second, the increase in ACL with increasing temperature is the result of a shift in the entire range of chain length, rather than proportional changes in one or two chain lengths.

Fig. 5A shows plant ACL values vs. mean annual temperature for plants, showing the general increase in ACL values with increasing temperature but also the large range of ACL values for plants at the same temperature. Regression results for all plant measurements were only significant ($p < 0.005$) for summer temperature (Table 1), and to test whether there are trends within species, Fig. 5B shows ACL values vs. summer temperature only for plant species or genera with two or more measurements. However, given the small sample size (2–6) there was no significant correlation within species. When plant ACL values were averaged by site for the 14 sites with more than one plant measurement, site-averaged ACL values correlated with mean summer temperature (Fig. 5C). In linear regressions, site-averaged ACL values correlated with mean annual temperature (R^2 0.44, p 0.010) and mean summer temperature (R^2 0.55, p 0.003). The strength of each of the regressions was similar to those between mean annual and summer temperature and soil ACL values, and the reduced significance was due to the reduced sample size.

Although we restricted annual precipitation, the seasonal distribution of precipitation varied across the transect, with northern sites receiving more summer precipitation than southern sites, so we also tested for correlations between ACL values and precipitation. ACL values did not correlate with annual precipitation for either soils or plants. Soil and plant ACL values also did not correlate with summer precipitation (June, July, August) when controlling for summer temperature. A similar lack of correlation between ACL values and precipitation existed for all other seasons (not reported). Relative humidity (values calculated only for annual and summer months) generally correlated negatively with mean temperature except for the most southern sites, which were near enough to the Gulf of Mexico to receive coastal moisture. We also tested soil ACL values against temperature, precipitation and relative humidity as partial correlations, where ACL values were correlated with one climate variable while controlling for the other two variables. This was done for summer and annual mean climate values. The partial correlation results show that temperature was consistently the strongest driver, having the largest correlation coefficients, and was the only significant driver with the exception of annual values of relative humidity (Table 2).

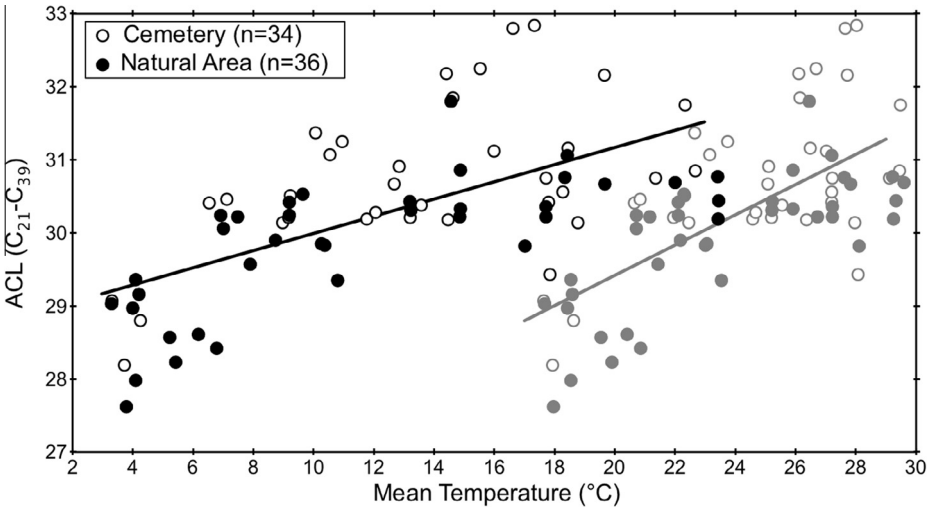

Fig. 3. ACL of soil *n*-alkanes, plotted by mean annual temperature (black points) and mean temperature of summer months (average of June, July and August, gray points). Solid lines are linear regression lines for all ACL data vs. mean annual temperature (black) and summer temperature (gray). Open circles represent samples from cemeteries and filled circles are samples from protected natural areas.

Table 1
Linear regression results for soil and plant ACL values by mean seasonal temperatures, including coefficients of determination (R^2) and significance values (p).[a]

ACL	Spring		Summer		Autumn		Winter		Annual	
	R^2	p	R^2	p	R^2	p	R^2	p	R^2	p
All soils	0.38	**	0.47	**	0.39	**	0.40	**	0.41	**
Cemetery	0.27	*	0.36	**	0.29	*	0.29	*	0.30	*
Natural area	0.48	**	0.55	**	0.48	**	0.51	**	0.50	**
Plants	0.11	0.014	0.15	*	0.11	0.013	0.12	0.011	0.12	0.010

[a] ** indicates $p < 0.001$ and * indicates $p < 0.005$; where $p \geqslant 0.005$, the value is given.

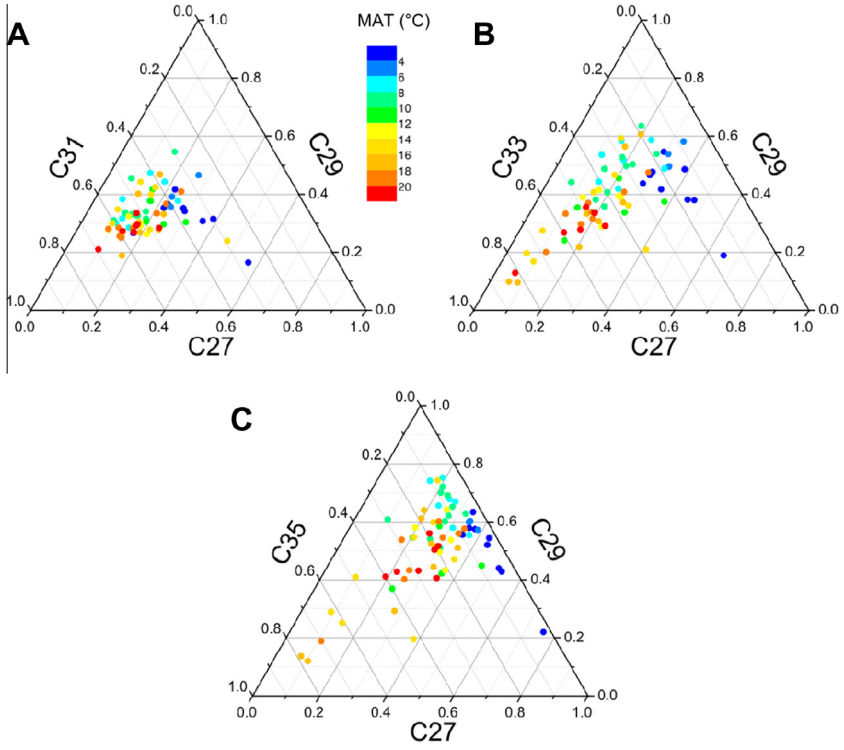

Fig. 4. Ternary diagrams of soil n-alkane relative chain length abundance, plotting the C_{27} and C_{29} chain lengths by (A) C_{31}, (B) C_{33} and (C) C_{35}. Sites are color-coded by mean annual temperature and legend applies to all three figures (for interpretation of the references to color in this figure legend, the reader is referred to the web version of the article).

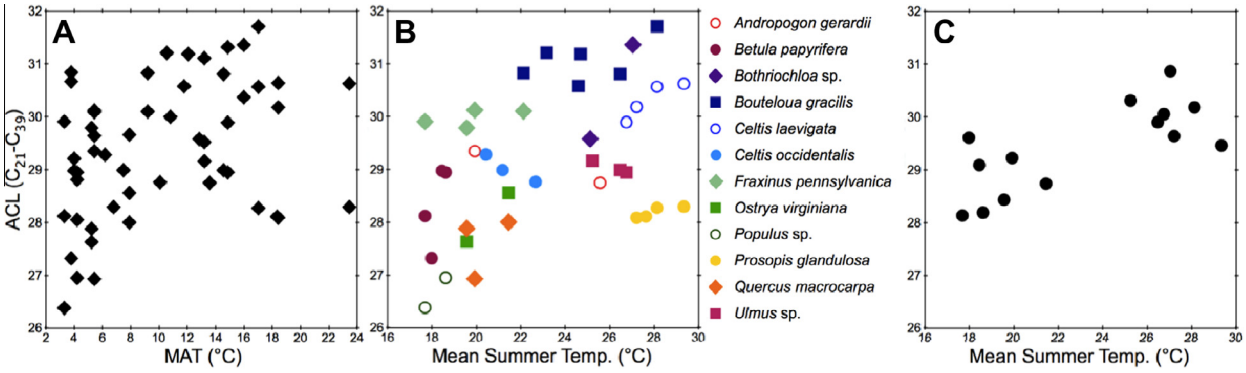

Fig. 5. (A) ACL for plants plotted by mean annual temperature (MAT). (B) Plant ACL values for all species or genera with two or more measurements plotted by mean summer temperature, with legend. (C) Plant ACL values averaged by site for sites with two or more plants measured plotted by mean summer temperature.

3.4. Soil n-alkane distributions and $\delta^{13}C$

Soil ACL values did not correlate with soil $\delta^{13}C$ values when all sites were considered (Fig. 6). When natural areas were considered alone, soil ACL values correlated with $\delta^{13}C$ values (R^2 0.31, $p < 0.001$) and there was no correlation for cemeteries. However, soil $\delta^{13}C$ values also correlated with mean summer temperature for these sites (R^2 0.33, $p < 0.001$) and when soil ACL values were regressed against both soil $\delta^{13}C$ values and mean summer temperature for natural area sites, the correlation with temperature

Table 2
Partial correlation results for soil ACL values ($n = 70$). Pearson product-moment correlation coefficient (r) and significance values (p)[a] for each parameter.

	June		July		August		Summer		Annual	
	r	p	r	p	r	p	r	p	r	p
Mean T	0.44	**	0.42	**	0.37	*	0.36	*	0.48	**
Precipitation	0.09	0.465	0.04	0.764	0.12	0.333	0.11	0.379	0.25	0.041
RH	−0.26	0.030	−0.19	0.130	−0.17	0.158	−0.22	0.067	−0.41	**

[a] ** indicates $p < 0.001$ and * indicates $p < 0.005$; where $p \geqslant 0.005$, the value is given.

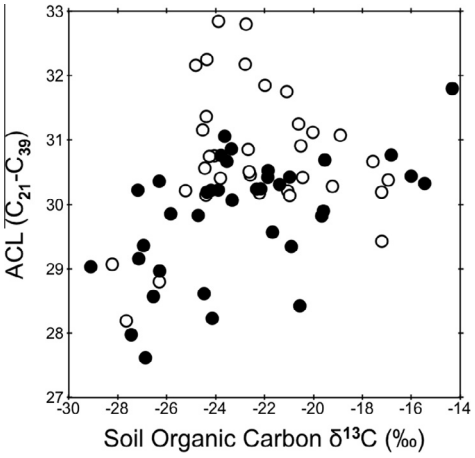

Fig. 6. ACL of soil *n*-alkanes plotted vs. $\delta^{13}C$ value of soil OC for natural areas (filled circles) and cemeteries (open circles).

remained significant (partial regression $p < 0.001$) and the correlation with soil $\delta^{13}C$ values disappeared (partial regression p 0.172). This analysis indicates that the correlation between soil ACL and $\delta^{13}C$ values in natural areas is the result of a common dependence of both ACL and $\delta^{13}C$ values on temperature.

4. Discussion

4.1. Climate influence on chain length distribution

Overall, *n*-alkane chain length distribution trended towards long chain length with warmer temperature, as demonstrated in Fig. 4. Soil ACL values across the transect correlated with both summer and mean annual temperature (Fig. 3), but did not correlate with soil $\delta^{13}C$ values (Fig. 6). The apparent correlation between ACL and $\delta^{13}C$ values in natural area soils (Fig. 6) reflects the common dependence of both on growing season temperature (Section 3.4). This suggests that input from C_4 plants was not a direct driver of the variation in ACL, at least for plants in North America. Longer chain lengths have been observed in association with C_4 savanna grasses in Africa (Rommerskirchen et al., 2006b). However, Vogts et al. (2009) observed that, within African C_3 woody plants, savanna (dry environment) species produced more C_{31} than rainforest (wet environment) species. Vogts et al. (2012) and Rommerskirchen et al. (2003) observed an increase in ACL, as well as $\delta^{13}C$ values, in marine sediments off the west coast of Africa, reflecting increasing input from arid, C_4-dominated terrestrial areas. Carr et al. (2010) saw an increase in C_{31} vs. C_{29} in a time sequence from rock hyrax middens in South Africa, a shift which they correlated with increasingly positive $\delta^{13}C$ values and increasing N isotope values, interpreted as indicators of C_4 plants and local aridity. Taken together, these studies demonstrate a general correlation, at least in Africa, between longer chain lengths, C_4 plants and arid conditions. Since, to our knowledge, there is no a priori reason why C_4 plants would synthesize longer chain lengths, it is possible that both C_4 photosynthesis and longer chain lengths are independently related to the same environmental factors, i.e. aridity and high temperature. It may be that increased temperature and/or aridity select independently for both C_4 photosynthesis and longer chain length. The range for soil $\delta^{13}C$ values here (−29.1‰ to −14.3‰) covers the spectrum (cf. Tieszen et al., 1979; O'Leary, 1988) of leaf $\delta^{13}C$ values for C_3 plants $\bar{x} = -28‰$ to C_4 plants $\bar{x} = -14‰$, suggesting that the soil OM here ranged from 100% C_3 plant input to nearly 100% C_4. Thus, the lack of correlation between soil ACL and $\delta^{13}C$ values here supports climate as an independent driver of both C_4 photosynthesis and longer chain length.

Plant *n*-alkanes exhibited a wider range of ACL values and a weaker correlation between ACL and temperature than soil *n*-alkanes (Figs. 3, 5A and B). This may be because the variation in *n*-alkane chain length distributions in individual plants, which likely has a strong genetic component, is pooled and averaged in soils, making the net influence of temperature more apparent. Indeed, different plant species likely do not respond to the same degree to environmental drivers. In a survey of arid plants and soils in South Africa, Carr et al. (2014) reported significant variability in the chain length distributions of plants across multiple environments, where one species appeared to be sensitive to environmental variation and another produced highly consistent distributions regardless of location. Although it is only a rough approximation of the integration of plant *n*-alkanes to a given soil, the stronger correlation between site-averaged plant ACL values and temperature here (Fig. 5C) demonstrates the effect of pooling multiple plant inputs. Soil *n*-alkanes are also likely biased towards plant species with high biomass turnover and/or high *n*-alkane production, whereas the plants that were sampled here represented only a portion of the local plant community for each site. Moreover, the sample size for individual plant species was relatively small ($n = 6$ for the most sampled species, *Bouteloua gracilis*), which may be too small to capture environmental influence within a single species.

Across a similar latitudinal transect along the eastern USA, Tipple and Pagani (2013) observed a correlation between temperature and ACL values for three common tree species. Other transect studies have observed correlations between growing temperature and chain length distributions in plants (Dodd and Poveda, 2003; Sachse et al., 2006) as well as soils and sediments (Leider et al., 2013). Although a more indirect measure, studies of atmospheric dust over the Pacific Ocean have also observed a correspondence between latitude and chain length, with higher ACL values at lower latitudes (Bendle et al., 2007), as well as an increase in ACL values from spring to summer (Gagosian and Peltzer, 1986). Quaternary paleoclimate studies of marine and lacustrine sediment archives have reported higher ACL values during warm interglacial periods and lower values in glacial periods (Hinrichs et al., 1997). Together with the findings here, these data support the hypothesis that temperature drives *n*-alkane chain length, and the correlation between soil ACL values and temperature reported here is one of the strongest of such correlations.

In addition to temperature, aridity has also been proposed as a driver of chain length, where drier conditions promote longer

chain length (Dodd et al., 1998; Andersson et al., 2011). A study of atmospheric dust off the western coast of Africa found lower ACL values from locations adjacent to rainforest and higher values from desert regions (Schefuß et al., 2003). However, the evidence for a correlation between aridity and *n*-alkane chain length distribution appears to be more mixed, and whether temperature or aridity is the primary driver of ACL change in sediment records may depend on the regional context. For example, Calvo et al. (2004) observed increased ACL values during dry but cooler time periods from Pleistocene sediments from the Tasman Sea. In contrast, Castañeda et al. (2009) observed increased ACL values from Lake Malawi sediments in warmer, wetter time periods through the Late Pleistocene. For modern plants, a recent study reported opposite trends in ACL in the leaves of two different genera with increasing aridity in Australia (Hoffmann et al., 2013), while another study of arid-adapted plants in South Africa reported a significant but weak positive correlation between aridity and ACL in plants and soils (Carr et al., 2014). Similar to the temperature results here, Carr et al. (2014) also found that the correlation between ACL and aridity was stronger for soils than for plants, again suggesting that soils exert an averaging effect on variation among plants. Our study shows only a correlation between soil ACL values and relative humidity when relative humidity was calculated for the entire year. Thus the evidence for aridity as a driver is not yet as clear as it is for temperature and calls for further investigation of modern environments. Overall, these and previous findings (Bush and McInerney, 2013) suggest that it may be prudent to interpret changes in chain length distributions during periods of climate change not as the direct result of plant community turnover per se (Schwark et al., 2002; Zhang et al., 2006; Bai et al., 2009) but rather a result of the climate conditions.

4.2. Mechanisms of temperature influence

Cuticular wax blocks non-stomatal leaf water loss and is a critical adaptation for land plants. Plants allocate a large portion of lipid synthesis to cuticular wax lipids (Samuels et al., 2008). It is therefore expected that wax amount, structure and composition would be adapted to minimize water loss, as well as serving other ecological functions (Hall and Jones, 1961; Shepherd and Griffiths, 2006; Mamrutha et al., 2010). Increasing temperature has been shown to increase the permeability of leaf cuticle surfaces, including at natural environmental temperature (Riederer and Schreiber, 2001; Riederer, 2006), and plants in hotter, drier environments synthesize less permeable cuticles (Schreiber and Riederer, 1996). Also, noting that leaf wax does not form a smooth surface over the leaf cuticle, but rather forms crystalline structures (Post-Beittenmiller, 1996), the loss of this crystal structure due to partial melting may negatively impact the ecological functions of leaf wax, e.g. mediating plant–insect and plant–microbe interactions (Riederer and Müller, 2006). Thus, it is reasonable to surmise that, under warm and/or arid conditions, selective pressures favor the production of longer, more hydrophobic *n*-alkane chain lengths (Shepherd and Griffiths, 2006). Furthermore, this functionality must be maintained at the warmest temperatures experienced by the plant, i.e. the warmest months of the growing season. This may explain why chain length correlates most strongly with summer temperature, even if leaf waxes are largely synthesized in spring at the beginning of the growing season (Tipple et al., 2013). Thus, although the isotope values of the *n*-alkanes reflect water uptake at the time of leaf wax synthesis and leaf flush (Kahmen et al., 2011; Tipple et al., 2013), *n*-alkane chain length distribution is decoupled from spring environmental conditions and instead reflects summer temperature. However, it is noted that, while this hypothesis may explain observations for deciduous and annual plants that produce and lose their leaves over the course of a single growing season, it may not hold for evergreen plants in cold climates, the leaves of which may require longer chain length to survive winter freezing and desiccation in dry, cold conditions (Dodd and Poveda, 2003). There is also a clear genetic or taxonomic component to *n*-alkane biosynthesis, where some species produce highly consistent chain length distributions across their range and some species are much more variable (Bush and McInerney, 2013; Carr et al., 2014) and the reasons for this are unclear. Data on the biosynthetic control and function of *n*-alkanes in leaf wax are sparse and the biochemistry of this relationship has yet to be fully explored.

4.3. Application to a paleoclimate archive: the Paleocene–Eocene Thermal Maximum

In order to test the applicability of the correlation between temperature and chain length to paleoclimate archives, we applied the findings to the Paleocene–Eocene Thermal Maximum (PETM). The PETM was an extreme, geologically brief, global warming event that occurred ca. 56×10^6 yr ago, before the evolution of C_4 plants, and that has been observed in multiple sedimentary archives (McInerney and Wing, 2011). Of the studies that have examined *n*-alkanes across the PETM, several discuss ACL values: Smith et al. (2007) for Wyoming, Handley et al. (2008) for Tanzania, Schouten et al. (2007) for the Arctic Ocean and Tipple et al. (2011) for Forada, Italy. In three of the four records, ACL increased at the onset of PETM warming (Schouten et al., 2007; Smith et al., 2007). In the fourth (Forada, Italy), ACL decreased at the onset of the PETM. The decrease was associated with a decrease in *n*-alkane δD values that might suggest that the area locally became wetter (Tipple et al., 2011), which in turn may have reduced the effect of increased temperature. Similarly, during the cooling and recovery phase of the PETM, three of the four records showed a decrease in ACL (Schouten et al., 2007; Smith et al., 2007; Tipple et al., 2011). Handley et al. (2008) speculated that the Tanzania record had a hiatus that spanned the recovery, so the ACL signal was not recorded for that interval. Although atmospheric CO_2 also increased at the onset of the PETM, a study of modern plants, in which *n*-alkane distributions were found not to change with elevated CO_2, suggests that this is unlikely to have had an effect on ACL values across the PETM (Wiesenberg et al., 2008). Thus, it is possible that the global warming, potentially coupled with drying in some areas, drove the increase in ACL observed in most records at the onset of the PETM, and conversely that the cooling at the end of the PETM largely drove a decrease in ACL. Other studies have already speculated on the effects of aridity and temperature on chain length distributions across Quaternary climate change events, e.g. glacial–interglacial cycles (Rommerskirchen et al., 2006a). Measures of variation in chain length distributions such as ACL may serve as useful qualitative indicators of climate change events, supplementing other proxy records.

5. Conclusions

This study demonstrates a strong correlation between summer temperature and *n*-alkane chain length distributions. Complemented by a previous study that showed a lack of correlation between *n*-alkane chain length and most major plant groups (Bush and McInerney, 2013) and in conjunction with other studies that show a correlation between chain length and aridity or temperature, this suggests that the spatial and temporal variation in chain length distribution may be driven in large part by growing season temperature and/or aridity. There is no evidence to support a direct link between C_4 photosynthesis and long chain length ($> C_{31}$), which suggests that they both are adaptations to hot and/

or dry environments. Lastly, soils integrate the various *n*-alkane signals from local plants, and therefore may provide a better comparison dataset for interpretation of sediments and paleosols. Future research would benefit from investigation of the mechanics of the incorporation of *n*-alkanes into cuticular wax and the effect of cuticle lipid composition on water permeability, as well as the nature of the relationship between leaf wax *n*-alkanes and their sources, and their incorporation into sediment and fossil archives.

Acknowledgements

We are grateful to the state and local agencies who provided access and assistance: Minnesota Department of Natural Resources, South Dakota Game, Fish & Parks Department, Nebraska Game and Parks Commission, Kansas Department of Wildlife, Parks and Tourism, Oklahoma Tourism and Recreation Department, Texas Parks & Wildlife Department, and Sabal Palms Sanctuary. Funding was provided by The Paleontological Society, Sigma Xi and EPA Science to Achieve Results (STAR) Graduate Fellowship to R.T.B. and by NSF EAR-1053351 and Australian Research Council FT110100793 to F.A.M. Portions of the work were presented at the GSA 2012 Annual Meeting, thanks to funding from the Association for Women Geoscientists. Thanks go to N. Richter and K. Dutta for laboratory assistance and to S. Wing, N. Blair and B. Sageman for insightful comments and suggestions. The manuscript was much improved by comments from two anonymous reviewers.

Appendix A. Supplementary data

Supplementary data associated with this article can be found, in the online version, at http://dx.doi.org/10.1016/j.orggeochem.2014.12.003.

Associate Editor—**P.A. Meyers**

References

Andersson, R.A., Kuhry, P., Meyers, P., Zebühr, Y., Crill, P., Mörth, M., 2011. Impacts of paleohydrological changes on *n*-alkane biomarker compositions of a Holocene peat sequence in the eastern European Russian Arctic. Organic Geochemistry 42, 1065–1075.

Bai, Y., Fang, X., Nie, J., Wang, Y., Wu, F., 2009. A preliminary reconstruction of the paleoecological and paleoclimatic history of the Chinese Loess Plateau from the application of biomarkers. Palaeogeography, Palaeoclimatology, Palaeoecology 271, 161–169.

Balesdent, J., Girardin, C., Mariotti, A., 1993. Site-related $\delta^{13}C$ of tree leaves and soil organic matter in a temperate forest. Ecology 74, 1713–1721.

Bendle, J., Kawamura, K., Yamazaki, K., Niwai, T., 2007. Latitudinal distribution of terrestrial lipid biomarkers and *n*-alkane compound-specific stable carbon isotope ratios in the atmosphere over the western Pacific and Southern Ocean. Geochimica et Cosmochimica Acta 71, 5934–5955.

Brincat, D., Yamada, K., Ishiwatari, R., Uemura, H., Naraoka, H., 2000. Molecular isotopic stratigraphy of long-chain *n*-alkanes in Lake Baikal Holocene and glacial age sediments. Organic Geochemistry 31, 287–294.

Buchmann, N., Kao, W.-Y., Ehleringer, J.R., 1997. Influence of stand structure on carbon-13 of vegetation, soils, and canopy air within deciduous and evergreen forests in Utah, United States. Oecologia 110, 109–119.

Bush, R.T., McInerney, F.A., 2013. Leaf wax *n*-alkane distributions in and across modern plants: implications for paleoecology and chemotaxonomy. Geochimica et Cosmochimica Acta 117, 161–179.

Calvo, E., Pelejero, C., Logan, G.A., De Deckker, P., 2004. Dust-induced changes in phytoplankton composition in the Tasman Sea during the last four glacial cycles. Paleoceanography 19, 1–10.

Carr, A.S., Boom, A., Chase, B.M., 2010. The potential of plant biomarker evidence derived from rock hyrax middens as an indicator of palaeoenvironmental change. Palaeogeography, Palaeoclimatology, Palaeoecology 285, 321–330.

Carr, A.S., Boom, A., Grimes, H.L., Chase, B.M., Meadows, M.E., Harris, A., 2014. Leaf wax *n*-alkane distributions in arid zone South African flora: environmental controls, chemotaxonomy and palaeoecological implications. Organic Geochemistry 67, 72–84.

Castañeda, I.S., Schouten, S., 2011. A review of molecular organic proxies for examining modern and ancient lacustrine environments. Quaternary Science Reviews 30, 2851–2891.

Castañeda, I.S., Werne, J.P., Johnson, T.C., Filley, T.R., 2009. Late Quaternary vegetation history of southeast Africa: the molecular isotopic record from Lake Malawi. Palaeogeography, Palaeoclimatology, Palaeoecology 275, 100–112.

Daly, C., Halbleib, M., Smith, J.I., Gibson, W.P., Doggett, M.K., Taylor, G.H., Curtis, J., Pasteris, P.P., 2008. Physiographically sensitive mapping of climatological temperature and precipitation across the conterminous United States. International Journal of Climatology 28, 2031–2064.

Dodd, R.S., Poveda, M.M., 2003. Environmental gradients and population divergence contribute to variation in cuticular wax composition in *Juniperus communis*. Biochemical Systematics and Ecology 31, 1257–1270.

Dodd, R.S., Rafii, Z.A., Power, A.B., 1998. Ecotypic adaptation in *Austrocedrus chilensis* in cuticular hydrocarbon composition. New Phytologist 138, 699–708.

Eglinton, G., Hamilton, R.J., 1967. Leaf epicuticular waxes. Science 156, 1322–1335.

Gagosian, R.B., Peltzer, E.T., 1986. The importance of atmospheric input of terrestrial organic material to deep sea sediments. Organic Geochemistry 10, 661–669.

Gustafson, D.J., Gibon, D.J., Nickrent, D.L., 2005. Using local seeds in prairie restoration. Native Plants 6, 25–28.

Hall, D.M., Jones, R.L., 1961. Physiological significance of surface wax on leaves. Nature 191, 95–96.

Handley, L., Pearson, P.N., McMillan, I.K., Pancost, R.D., 2008. Large terrestrial and marine carbon and hydrogen isotope excursions in a new Paleocene/Eocene boundary section from Tanzania. Earth and Planetary Science Letters 275, 17–25.

Hinrichs, K.-U., Rinna, J., Rullkötter, J., 1997. Late Quaternary paleoenvironmental conditions indicated by marine and terrestrial molecular biomarkers in sediments from the Santa Barbara Basin. Interagency Ecological Program for the Sacramento-San Joaquin Estuary Technical Report 57, 125–137.

Hoffmann, B., Kahmen, A., Cernusak, L.A., Arndt, S.K., Sachse, D., 2013. Abundance and distribution of leaf wax *n*-alkanes in leaves of Acacia and Eucalyptus trees along a strong humidity gradient in northern Australia. Organic Geochemistry 62, 62–67.

Kahmen, A., Dawson, T.E., Vieth, A., Sachse, D., 2011. Leaf wax *n*-alkane δD values are determined early in the ontogeny of *Populus trichocarpa* leaves when grown under controlled environmental conditions. Plant, Cell & Environment 34, 1639–1651.

Kawamura, K., Ishimura, Y., Yamazaki, K., 2003. Four years' observations of terrestrial lipid class compounds in marine aerosols from the western North Pacific. Global Biogeochemical Cycles 17, 1–19.

Leider, A., Hinrichs, K.-U., Schefuß, E., Versteegh, G.J.M., 2013. Distribution and stable isotopes of plant wax derived *n*-alkanes in lacustrine, fluvial and marine surface sediments along an Eastern Italian transect and their potential to reconstruct the hydrological cycle. Geochimica et Cosmochimica Acta 117, 16–32.

Mamrutha, H.M., Mogili, T., Lakshmi, K.J., Rama, N., Kosma, D., Kumar, M.U., Jenks, M.A., Nataraja, K.N., 2010. Leaf cuticular wax amount and crystal morphology regulate post-harvest water loss in mulberry (*Morus* species). Plant Physiology and Biochemistry 48, 690–696.

Marzi, R., Torkelson, B.E., Olson, R.K., 1993. A revised carbon preference index. Organic Geochemistry 20, 1303–1306.

McInerney, F.A., Wing, S.L., 2011. The Paleocene–Eocene thermal maximum: a perturbation of carbon cycle, climate, and biosphere with implications for the future. Annual Review of Earth and Planetary Sciences 39, 489–516.

Medeiros, P.M., Simoneit, B.R.T., 2007. Gas chromatography coupled to mass spectrometry for analyses of organic compounds and biomarkers as tracers for geological, environmental, and forensic research. Journal of Separation Science 30, 1516–1536.

Melillo, J.M., Aber, J.D., Linkins, A.E., Ricca, A., Fry, B., Nadelhoffer, K.J., 1989. Carbon and nitrogen dynamics along the decay continuum: plant litter to soil organic matter. Plant and Soil 115, 189–198.

O'Leary, M.H., 1988. Carbon isotopes in photosynthesis. BioScience 38, 328–336.

Post-Beittenmiller, D., 1996. Biochemistry and molecular biology of wax production in plants. Annual Review of Plant Physiology and Plant Molecular Biology 47, 405–430.

Riederer, M., 2006. Thermodynamics of the water permeability of plant cuticles: characterization of the polar pathway. Journal of Experimental Botany 57, 2937–2942.

Riederer, M., Müller, C., 2006. Biology of the Plant Cuticle. Blackwell, Oxford.

Riederer, M., Schreiber, L., 2001. Protecting against water loss: analysis of the barrier properties of plant cuticles. Journal of Experimental Botany 52, 2023–2032.

Rommerskirchen, F., Eglinton, G., Dupont, L., Günter, U., Wenzel, C., Rullkötter, J., 2003. A north to south transect of Holocene southeast Atlantic continental margin sediments: relationship between aerosol transport and compound-specific $\delta^{13}C$ land plant biomarker and pollen records. Geochemistry Geophysics Geosystems 4, 1101–1128.

Rommerskirchen, F., Eglinton, G., Dupont, L., Rullkötter, J., 2006a. Glacial/interglacial changes in southern Africa: compound-specific $\delta^{13}C$ land plant biomarker and pollen records from southeast Atlantic continental margin sediments. Geochemistry Geophysics Geosystems 7, 1–2.

Rommerskirchen, F., Plader, A., Eglinton, G., Chikaraishi, Y., Rullkötter, J., 2006b. Chemotaxonomic significance of distribution and stable carbon isotopic composition of long-chain alkanes and alkan-1-ols in C_4 grass waxes. Organic Geochemistry 37, 1303–1332.

Sachse, D., Radke, J., Gleixner, G., 2006. ΔD values of individual n-alkanes from terrestrial plants along a climatic gradient – implications for the sedimentary biomarker record. Organic Geochemistry 37, 469–483.

Sachse, D., Billault, I., Bowen, G.J., Chikaraishi, Y., Dawson, T.E., Feakins, S.J., Freeman, K.H., Magill, C.R., McInerney, F.A., van der Meer, M.T.J., Polissar, P., Robins, R.J., Sachs, J.P., Schmidt, H.-L., Sessions, A.L., White, J.W.C., West, J.B., Kahmen, A., 2012. Molecular paleohydrology: interpreting the hydrogen-isotopic composition of lipid biomarkers from photosynthesizing organisms. Annual Review of Earth and Planetary Sciences 40, 221–249.

Samuels, L., Kunst, L., Jetter, R., 2008. Sealing plant surfaces: cuticular wax formation by epidermal cells. Annual Review of Plant Biology 59, 683–707.

Schefuß, E., Schouten, S., Jansen, J.H.F., Sinninghe Damsté, J.S., 2003. African vegetation controlled by tropical sea surface temperatures in the mid-Pleistocene period. Nature 422, 418–421.

Schouten, S., Woltering, M., Rijpstra, W.I.C., Sluijs, A., Brinkhuis, H., Sinninghe Damsté, J.S., 2007. The Paleocene–Eocene carbon isotope excursion in higher plant organic matter: differential fractionation of angiosperms and conifers in the Arctic. Earth and Planetary Science Letters 258, 581–592.

Schreiber, L., Riederer, M., 1996. Ecophysiology of cuticular transpiration: comparative investigation of cuticular water permeability of plant species from different habitats. Oecologia 107, 426–432.

Schwark, L., Zink, K., Lechterbeck, J., 2002. Reconstruction of postglacial to early Holocene vegetation history in terrestrial Central Europe via cuticular lipid biomarkers and pollen records from lake sediments. Geology 30, 463–466.

Shepherd, T., Griffiths, D.W., 2006. The effects of stress on plant cuticular waxes. New Phytologist 171, 469–499.

Smith, F.A., Wing, S.L., Freeman, K.H., 2007. Magnitude of the carbon isotope excursion at the paleocene–eocene thermal maximum: the role of plant community change. Earth and Planetary Science Letters 262, 50–65.

Sorensen, J.T., Holden, D.J., 1974. Germination of native prairie forb seeds. Journal of Range Management 27, 123–126.

Still, C.J., Berry, J.A., Collatz, G.J., DeFries, R.S., 2003. Global distribution of C_3 and C_4 vegetation: carbon cycle implications. Global Biogeochemical Cycles 17, 1–14.

Teeri, J.A., Stowe, L.G., 1976. Climatic patterns and the distribution of C_4 grasses in North America. Oecologia 23, 1–12.

Tieszen, L.L., Senyimba, M.M., Imbamba, S.K., Troughton, J.H., 1979. The distribution of C_3 and C_4 grasses and carbon isotope discrimination along an altitudinal and moisture gradient in Kenya. Oecologia 37, 337–350.

Tieszen, L.L., Reed, B.C., Bliss, N.B., Wylie, B.K., DeJong, D.D., 1997. NDVI, C_3 and C_4 production, and distributions in Great Plains grassland land cover classes. Ecological Applications 7, 59–78.

Tipple, B.J., Pagani, M., 2013. Environmental control on eastern broadleaf forest species' leaf wax distributions and D/H ratios. Geochimica et Cosmochimica Acta 111, 64–77.

Tipple, B.J., Pagani, M., Krishnan, S., Dirghangi, S.S., Galeotti, S., Agnini, C., Giusberti, L., Rio, D., 2011. Coupled high-resolution marine and terrestrial records of carbon and hydrologic cycles variations during the paleocene–eocene thermal maximum (PETM). Earth and Planetary Science Letters 311, 82–92.

Tipple, B.J., Berke, M.A., Doman, C.E., Khachaturyan, S., Ehleringer, J.R., 2013. Leaf-wax *n*-alkanes record the plant-water environment at leaf flush. Proceedings of the National Academy of Sciences United States of America 110, 2659–2664.

Vogts, A., Moossen, H., Rommerskirchen, F., Rullkötter, J., 2009. Distribution patterns and stable carbon isotopic composition of alkanes and alkan-1-ols from plant waxes of African rain forest and savanna C_3 species. Organic Geochemistry 40, 1037–1054.

Vogts, A., Schefuß, E., Badewein, T., Rullkötter, J., 2012. *n*-Alkane parameters from a deep sea sediment transect off southwest Africa reflect continental vegetation and climate conditions. Organic Geochemistry 47, 109–119.

Wang, Y.V., Larsen, T., Leduc, G., Andersen, N., Blanz, T., Schneider, R.R., 2013. What does leaf wax δD from a mixed C_3/C_4 vegetation region tell us? Geochimica et Cosmochimica Acta 111, 128–139.

Wiesenberg, G.L.B., Schmidt, M.W.I., Schwark, L., 2008. Plant and soil lipid modifications under elevated CO_2 conditions. I. Lipid distribution patterns. Organic Geochemistry 39, 91–102.

Zhang, Z., Zhao, M., Eglinton, G., Lu, H., Huang, C.-Y., 2006. Leaf wax lipids as paleovegetational and paleoenvironmental proxies for the Chinese Loess Plateau over the last 170 kyr. Quaternary Science Reviews 25, 575–594.